Crystal Structure, Physical Properties, and Hydrolysis Kinetics of $[(O)(tmpa)V^{IV}(\mu\text{-}O)V^{V}(tmpa)(O)]^{3+}$

Robert A. Holwerda* and Bruce R. Whittlesey

Department of Chemistry and Biochemistry, Texas Tech University, Lubbock, Texas 79409

Mark J. Nilges

Illinois EPR Research Center, University of Illinois, Urbana, Illinois 61801

Received August 7, 1997

We report the synthesis, crystal structure, physical properties and hydrolysis kinetics of $[(O)(tmpa)V^{IV}(\mu\text{-}O)V^{V}(tmpa)(O)]^{3+}$ (tmpa = tris(2-pyridylmethyl)amine), the first cation in its class for which both solid state and solution-phase characteristics are fully consistent with expectations for a Robin−Day type III mixed-valence complex. $[V_2(tmpa)_2(O)_3](ClO_4)_3\cdot CH_3CN$ crystallizes in the triclinic, $P\bar{1}$ (No. 2) space group with $a = 10.719(2)$ Å, $b = 11.609(1)$ Å, $c = 19.516(2)$ Å, $\alpha = 87.876(9)°$, $\beta = 79.295(9)°$, $\gamma = 68.743(9)°$, and $V = 2222.6(6)$ Å^3; $Z = 2$. The two vanadium centers are crystallographically equivalent in a linear, oxo-bridged cation with V−O$_b$ and V=O bond lengths of 1.800(1) and 1.597(4) Å, respectively. A 15-hyperfine line EPR spectrum ($g = 1.9704$, $A = 46.4 \times 10^{-4}$ cm^{-1}) was observed for $[V_2(tmpa)_2(O)_3]^{3+}$, consistent with coupling of a single electron to two equivalent ^{51}V atoms. The mixed-valence complex exhibits an intervalence transfer (IT) band at 1.05×10^4 cm^{-1} ($\epsilon = 2.1 \times 10^3$ M^{-1} cm^{-1}, CH_3CN) whose energy is insensitive to variations in the solvent; d−d transitions are observed at 1.25×10^4 cm^{-1} ($^2E \leftarrow {}^2B_2$) and 1.44×10^4 cm^{-1} ($^2B_1 \leftarrow {}^2B_2$). $[V_2(tmpa)_2(O)_3]^{2+}$, $[V_2(tmpa)_2(O)_3]^{3+}$, and $[V_2(tmpa)_2(O)_3]^{4+}$ comprise a redox family related by vanadium (IV,V/IV,IV) and (V,V/IV,V) half-wave reduction potentials of 0.25 and 1.62 V vs NHE (25 °C, CH_3CN, $I = 0.1$ M), respectively. The hydrolysis reaction: $[V_2(tmpa)_2(O)_3]^{3+} + H_2O \rightarrow [V^{IV}(tmpa)(O)(OH)]^+ + [V^{V}(tmpa)(O)_2]^+ + H^+$ proceeds with an acid-independent rate constant of 2.37×10^{-3} s^{-1} (25 °C; $\Delta H^{\ddagger} = 71$ kJ/mol, $\Delta S^{\ddagger} = -59$ J/mol K). $[V_4O_5(tmpa)_4\{Fe(CN)_6\}](ClO_4)_4\cdot H_2O$ was isolated as an unexpected product from the reaction of $[V_2(tmpa)_2(O)_3](ClO_4)_2\cdot 2H_2O$ with equimolar $K_3[Fe(CN)_6]$ in aqueous solution. It is proposed that pairs of V^{IV}=O and V^{V}=O units aggregate with $[Fe(CN)_6]^{4-}$ into a charge transfer complex. Hexacyanoferrate(II)-to-vanadium IT charge transfer bands are observed at 1.98×10^4 cm^{-1} ($\epsilon = 5.3 \times 10^3$ M^{-1} cm^{-1}) and 2.72×10^4 cm^{-1} ($\epsilon = 9.3 \times 10^3$ M^{-1} cm^{-1}); a 29-line EPR spectrum ($g = 1.9737$, $A = 22.0 \times 10^{-4}$ cm^{-1}) demonstrates equal delocalization of unpaired electron density over all four V atoms (CH_3CN solution).

Introduction

A variety of dinuclear, oxo-bridged $V^{IV/V}$ complexes has been reported,[1−10] including examples which fall into Robin and Day[11] classes I, II, and III. To date, the only $V_2O_3^{3+}$ systems known to exhibit full delocalization of the single 3d electron over both vanadium atoms in the solid state have *N*-(2-hydroxyethyl)iminodiacetate ($Hidta^{2-}$)[1] or nitrilotriacetate (nta^{3-})[4] complementary ligands. The high susceptibility of these and related $V^{IV}-O-V^{V}$ complexes toward solvolytic cleavage of a $V-\mu-O^{2-}$ bond has made it difficult to establish whether type III behavior is retained in the solution phase. The presence of exactly equivalent vanadium centers would be indicated by a centrosymmetric crystal structure, a 15-line EPR signal arising from electron spin coupling to two ^{51}V ($I = {}^7/_2$) atoms, and an intervalence charge-transfer transition whose energy is insensitive to the solvent dielectric constant.[12] We report the synthesis, crystal structure, physical properties, and hydrolysis kinetics of $[(O)(tmpa)V^{IV}(\mu\text{-}O)V^{V}(tmpa)(O)]^{3+}$ (tmpa = tris(2-pyridylmethyl)amine), the first cation in its class for which both solid-state and solution-phase characteristics are fully consistent with expectations for a type III complex.

Experimental Section

Reagent grade chemicals and solvents were used throughout. Nitrosonium tetrafluoroborate and *N*-(n-$C_4H_9)_4ClO_4$ were used as supplied by Aldrich and GFS Chemicals, respectively. $[V(tmpa)(O)]_2O(ClO_4)_2\cdot 2H_2O$ (**1**)[13] and $[Co(phen)_3](ClO_4)_3\cdot 2H_2O$[14] were prepared by literature methods.

(1) Mahroof-Tahir, M.; Keramidas, A. D.; Goldfarb, R. B.; Anderson, O. P.; Miller, M. M.; Crans, D. C. *Inorg. Chem.* **1997**, *36*, 1657.
(2) Babonneau, F.; Sanchez, C.; Livage, J.; Launey, J.-P.; Daoudi, M.; Jeannin, Y. *Nouv. J. Chim.* **1982**, *6*, 353.
(3) Launay, J.-P.; Jeannin, Y.; Daoudi, M. *Inorg. Chem.* **1985**, *24*, 1052.
(4) Nishizawa, M.; Hirotsu, K.; Ooi, S.; Saito, K. *J. Chem. Soc., Chem. Commun.* **1979**, 707.
(5) Kojima, A.; Okazaki, K.; Ooi, S.; Saito, K. *Inorg. Chem.* **1983**, *22*, 1168.
(6) Riechel, T. L.; Sawyer, D. T. *Inorg. Chem.* **1975**, *14*, 1869.
(7) Pessoa, J. C.; Silva, J. A. L.; Vieira, A. L.; Vilas-Boas, L.; O'Brien, P.; Thornton, P. *J. Chem. Soc., Dalton Trans.* **1993**, 2857.
(8) Dutta, S.; Basu, P.; Chakravorty, A. *Inorg. Chem.* **1993**, *32*, 5343.
(9) Mondal, S.; Ghosh, P.; Chakravorty, A. *Inorg. Chem.* **1997**, *36*, 59.
(10) Oyaizu, K.; Yamamoto, K.; Yoneda, K.; Tsuchida, E. *Inorg. Chem.* **1996**, *35*, 6634.
(11) Robin, M. B.; Day, P. *Adv. Inorg. Chem. Radiochem.* **1967**, *10*, 247.
(12) Lever, A. B. P. *Inorganic Electronic Spectroscopy*, 2nd ed.; Elsevier: Amsterdam, 1984.
(13) Toftlund, H.; Larsen, S.; Murray, K. S. *Inorg. Chem.* **1991**, *30*, 3964.

S0020-1669(97)00983-X CCC: $15.00
Published on Web 01/12/1998

Caution! Perchlorate salts are potentially explosive and should be handled in small quantities.

Microanalyses were performed by Desert Analytics. Electronic spectra were acquired with Shimadzu UV-260 and UV-1601 (900−1100 nm) spectrophotometers. Infrared spectroscopy was carried out on a Perkin-Elmer model 1600 spectrophotometer. Cyclic voltammograms (Pt working and auxiliary electrodes, SCE reference electrode) were acquired with a Bioanalytical Systems CV-27 Voltammograph. Potential values were converted to the NHE scale by using (hydroxyethyl)ferrocene ($E_{1/2}$ = 402 mV vs NHE) as a calibrant. Electron paramagnetic resonance experiments were performed on a Varian E-122 X-band (9.53 GHz) spectrometer at a microwave power of 2.0 mW and a modulation amplitude of 4.0 gauss at 100 KHz. Second-derivative spectra were obtained by digital differentiation. The magnetic field was calibrated with a Varian NMR Gauss meter, and the microwave frequency was determined with a frequency meter. Hyperfine and *g* factor values were refined with spectral simulation (not shown). Measurements of $[H^+]$ generated through the hydrolysis of $[V_2(tmpa)_2(O)_3]^{3+}$ in 0.1 M $NaNO_3$ (CO_2-free) were made with a Brinkmann pH 104 meter, correcting pH readings for the activity of the medium.[15] The hydrolysis rate of $[V_2(tmpa)_2(O)_3]^{3+}$ (0.3 mM) was monitored through the 850 nm absorbance decrease in a thermostated, 1 cm path length cell. Runs were initiated by injecting 0.1 mL of a $[V_2(tmpa)_2(O)_3]^{3+}$ stock solution (CH_3CN) into 3.0 mL of aqueous HNO_3, maintaining constant ionic strength with $NaNO_3$. Pseudo-first-order rate constants (k_{obsd}) were calculated as the least-squares slopes of $\ln(A_t - A_\infty)$ vs time plots that were linear over ≥95% of ΔA_{850}. Reported values are generally the mean of two independent determinations.

$[V_2O_3(tmpa)_2](ClO_4)_3$ (2) and $[V_2O_3(tmpa)_2](ClO_4)_4\cdot 4H_2O$ (3). $NOBF_4$ (0.38 g) was mixed with **1** (1.0 g) and *N*-(*n*-Bu)$_4ClO_4$ (0.39 g) dissolved in 20 mL of stirred, dry acetonitrile at ambient temperature. Excess $NOBF_4$ was filtered off subsequent to a rapid color change from purple to blue, and the product was immediately precipitated by slow addition of diethyl ether. An insoluble green impurity was removed by filtration after redissolving the crude product in acetonitrile. The purified complex was precipitated with ether, washed with ether, and air-dried. Yield: 0.64 g. Anal. Calcd for $[V_2O_3(N_4C_{18}H_{18})_2](ClO_4)_3$ (**2**): C, 42.02; H, 3.53; N, 10.89. Found: C, 41.97; H, 3.56; N, 11.10. IR (KBr pellet): 3448 m, 1610 s, 1490 w, 1444 m, 1293 w, 1086 vs (ClO_4^-), 1032 w, 969 m (V═O), 909 w, 767 m, 623 s cm^{-1}. The dihydrate of **2** was prepared by the same method, except that the acetonitrile solution was mixed with 50 mL of 0.1 M $LiClO_4$ following removal of the green impurity. A blue powder (0.77 g) was collected after evaporation of CH_3CN and digestion for 2 days. Calcd for $[V_2O_3(N_4C_{18}H_{18})_2](ClO_4)_3\cdot 2H_2O$: C, 40.60; H, 3.79; N, 10.52. Found: C, 40.44; H, 3.65; N, 10.26. IR (KBr pellet): 3440 s, 1608 m, 1480 w, 1447 m, 1290 w, 1094 vs, 1032 w, 968 m, 941 w, 910 m, 770 m, 623 s cm^{-1}. An oxo-bridged divanadium(V) product was isolated when the reaction time was extended to 6 h. The same mixture of **1**, $NOBF_4$, and *N*-(*n*-Bu)$_4ClO_4$ employed in the synthesis of **2** slowly changed color from blue to pale green over several hours at room temperature. The green product was precipitated with ether after removal of excess $NOBF_4$, washed with ether, and air-dried. Anal. Calcd for $[V_2O_3(N_4C_{18}H_{18})_2](ClO_4)_4\cdot 4H_2O$ (**3**): C, 36.02; H, 3.69; N, 9.33. Found: C, 35.98; H, 3.61; N, 9.14. IR (KBr pellet): 3448 m, 3049 m, 1616 s, 1534 m, 1463 m, 1443 w, 1384 w, 1294 w, 1122 vs, 1084 vs (ClO_4^-), 1032 w, 974 m (V═O), 780 s, 625 m cm^{-1}.

$[V_4O_5(tmpa)_4\{Fe(CN)_6\}](ClO_4)_4.H_2O$ (4). An attempt to prepare **2** through the oxidation of **1** with equimolar hexacyanoferrate(III) in aqueous solution afforded instead a $V^{IV/V}$ charge-transfer complex with $[Fe(CN)_6]^{4-}$. **1** (2.0 g) dissolved in 50 mL of CH_3CN was mixed with $K_3[Fe(CN)_6]$ (0.70 g) and $LiClO_4$ (2.0 g) in 50 mL of water. An immediate color change from purple to deep red-orange was observed. Evaporation of CH_3CN gave an oily product which slowly converted to a red powder with stirring for 2 h. The crude product was purified by extraction into CH_3CN, leaving behind a salmon-colored residue. Evaporation of acetonitrile gave a dark red-orange, microcrystalline product. Yield: 0.65 g. Anal. Calcd for $[V_4O_5(N_4C_{18}H_{18})_4\{Fe(CN)_6\}](ClO_4)_4\cdot H_2O$ (**4**): C, 45.19; H, 3.60; N, 14.86. Found: C, 45.17; H, 3.68; N, 14.92. IR (KBr pellet): 3448 vs, 2056 vs (C≡N), 1610 s, 1490 w, 1444 m, 1293 w, 1094 vs (ClO_4^-), 1031 w, 981 m (V═O), 907 w, 769 m, 623 s cm^{-1}.

(14) Schilt, A. A.; Taylor, R. C. *J. Inorg. Nucl. Chem.* **1959**, *9*, 211.
(15) Gafford, B. G.; Holwerda, R. A. *Inorg. Chem.* **1989**, *28*, 60.

Table 1. Crystallographic Data for $[(tmpa)VO(\mu\text{-}O)VO(tmpa)](ClO_4)_3\cdot CH_3CN$

empirical formula	$C_{38}H_{39}Cl_3N_9O_{15}V_2$
fw	2770.06
space group	triclinic, $P\bar{1}$ (No. 2)
a, Å	10.719(2)
b, Å	11.609(1)
c, Å	19.516(2)
α, deg	87.876(9)
β, deg	79.295(9)
γ, deg	68.743(9)
volume, Å^3	2222.6(6)
Z	2
temperature, °C	−100
λ, Å (Mo Kα)	0.71073
ρ(calcd), g cm^{-3}	1.599
μ(Mo Kα), cm^{-1}	6.8
R^a	0.0636
$R_w{}^b$	0.0851

^{a} $R = \sum(|F_o| - |F_c|)/\sum|F_o|$. ^{b} $R_w = [\sum w(|F_o| - |F_c|)^2/\sum w|F_o|^2]^{1/2}$; $w = 1/\sigma^2(F)$.

Table 2. Selected Bond Lengths (Å) and Angles (deg) for $[(tmpa)VO(\mu\text{-}O)VO(tmpa)](ClO_4)_3\cdot CH_3CN$

V(1)−O(1)	1.597(4)	V(1)−O(2)	1.800(1)
V(1)−N(1)	2.082(5)	V(1)−N(2)	2.077(4)
V(1)−N(3)	2.156(4)	V(1)−N(4)	2.258(5)
O(1)−V(1)−O(2)	105.0(1)	O(1)−V(1)−N(1)	102.0(2)
O(2)−V(1)−N(1)	89.0(1)	O(1)−V(1)−N(2)	103.2(2)
O(2)−V(1)−N(2)	89.8(1)	N(1)−V(1)−N(2)	154.3(2)
O(1)−V(1)−N(3)	90.9(2)	O(2)−V(1)−N(3)	164.1(1)
N(1)−V(1)−N(3)	88.0(2)	N(2)−V(1)−N(3)	86.3(2)
O(1)−V(1)−N(4)	166.5(2)	O(2)−V(1)−N(4)	88.6(1)
N(1)−V(1)−N(4)	77.1(2)	N(2)−V(1)−N(4)	77.3(2)
N(3)−V(1)−N(4)	75.7(2)	V(1)−O(2)−V(1′)	180.0(1)

Crystallography. Crystals of $[V_2(tmpa)_2(O)_3](ClO_4)_3\cdot CH_3CN$ were grown by ether diffusion into an acetonitrile solution of **2**. The complex crystallized in space group $P\bar{1}$ (No. 2) with two molecules per unit cell (two half-molecules per asymmetric unit). Data were collected on a Siemens model P4 automated diffractometer using graphite-monochromated Mo Kα radiation. The unit cell parameters were determined and refined by a least-squares fit of 37 reflections. Data were corrected for Lorenz and polarization effects, and a semiempirical absorption correction based on *ψ* scans was applied. The space group determination was based upon the Laue symmetry and confirmed by solution of the structure. The structure was determined by direct methods followed by successive cycles of full-matrix least-squares refinement and difference Fourier analysis using the SHELXTL-IRIS software package provided by Siemens Analytical X-ray Instruments, Inc. The parameters refined included atomic coordinates and anisotropic thermal parameters for all non-hydrogen atoms. All three of the perchlorate anions exhibited positional disorder, which led to the poor *R* factors. The ORTEP drawing is shown with 30% probability ellipsoids. Crystallographic data and refinement details are given in Table 1. Table 2 presents selected bond lengths and angles.

Results and Discussion

The diamagnetic $V^{IV/IV}$ complex $[V(tmpa)(O)]_2O^{2+}$ (**1**) is linear with V−O (bridge) and V═O bond distances of 1.804 and 1.616 Å, respectively.[13] The cyclic voltammogram of **1** in dry CH_3CN has a reversible oxidation wave corresponding to the formation of a mixed-valence $V^{IV/V}$ species ($E_{1/2}$(IV,V/IV,IV) = 0.25 V vs NHE; ΔE_p = 71 mV) and a second, quasi-reversible oxidation wave ($E_{1/2}$(V,V/IV,V) = 1.62 V vs NHE; ΔE_p = 177 mV) for removal of a second electron (25

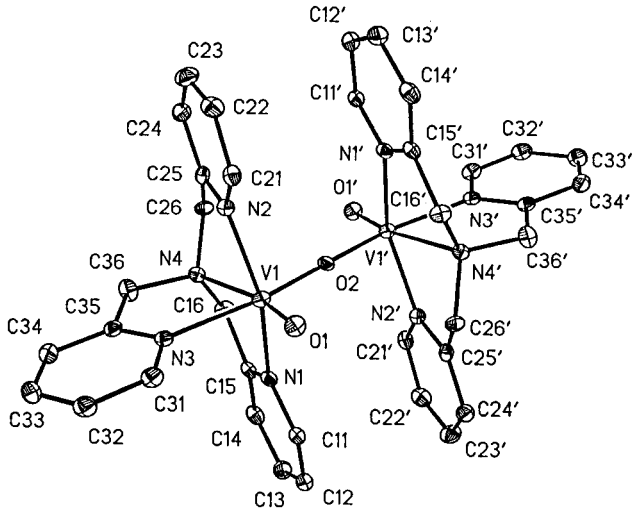

Figure 1. ORTEP diagram of the dinuclear cation in $[V_2(tmpa)_2(O)_3](ClO_4)_3 \cdot CH_3CN$. Hydrogen atoms have been omitted for clarity.

°C, 0.1 M *N*-(*n*-Bu)$_4$ClO$_4$, 50 mV/s sweep rate). A visible spectrophotometric titration of 0.10 mM $[V(tmpa)(O)]_2O^{2+}$ (λ_{max} = 533 nm, $\epsilon = 1.0 \times 10^4$ M^{-1} cm^{-1}) with $[Co(phen)_3]^{3+}$ ($E_{1/2}(Co^{III/II}) = 0.40$ V) in CH_3CN showed that bleaching of the purple divanadium(IV) reactant is accomplished upon removal of 1.03 ± 0.05 electron in the first oxidation step, consistent with the electrochemical finding. The mixed-valence complex is thermodynamically favored over a mixture of its $V^{IV/IV}$ and $V^{V/V}$ analogs; $K_c = 1.4 \times 10^{23}$ (25 °C) for the comproportionation reaction: $[V(tmpa)(O)]_2O^{2+} + [V(tmpa)(O)]_2O^{4+} \rightleftarrows 2[V(tmpa)(O)]_2O^{3+}$.

Syntheses of the blue $[V(tmpa)(O)]_2O^{3+}$ and green $[V(tmpa)(O)]_2O^{4+}$ cations were readily accomplished through oxidations of **1** with $NOBF_4$ in acetonitrile solution. Elemental analyses of **2** and **3** are in excellent agreement with the proposed formulas; infrared spectra show the expected small increases in ν(V=O) relative to that of **1** (943 cm^{-1}).[13] $E_{1/2}$(IV,V/IV,IV) and $E_{1/2}$(V,V/IV,V) values calculated from cyclic voltammograms of **2** and **3** were identical to those characteristic of **1**, confirming that these three complexes comprise a redox family. Although the V−O−V asymmetric stretching vibration was observed at 807 cm^{-1} for **1**, this feature was not seen in the infrared spectra of **2** and **3**. The crystal structure of **2**·CH_3CN (Figure 1) demonstrates that the two vanadium centers are crystallographically equivalent in a centrosymmetric, oxo-bridged cation with bonding lengths and angles similar to those reported for **1**.[13] Thus, the distorted octahedral N_4O_2 coordination spheres of vanadium in both **1** and **2** feature terminal V=O bonds trans to tmpa apical nitrogen atoms and cis to the V−O−V unit. As expected, the V−N and V−O bonds of **2** are slightly shorter (by 0.01−0.04 Å) than those of the divanadium(IV) complex, with the largest differences being seen in V−pyridyl N bonds that are cis to both the μ−O^{2-} and V=O groups. The ambient temperature X-band EPR spectrum of **2** in acetonitrile solution (Figure 2) exhibits the 15-hyperfine line pattern anticipated for coupling of a single electron to two equivalent ^{51}V atoms; $g = 1.9704$ and $A = 46.4 \times 10^{-4}$ cm^{-1} (139.2 MHz). Asymmetry of the lines may be due to incomplete motional averaging of the hyperfine tensor or **g** tensor anisotropy. A new eight-line pattern with $g = 1.9711$ and $A = 91.0 \times 10^{-4}$ cm^{-1} (272.8 MHz) slowly grows in when solutions of **2** absorb moisture from the air, generating a monomeric V^{IV} decomposition product.

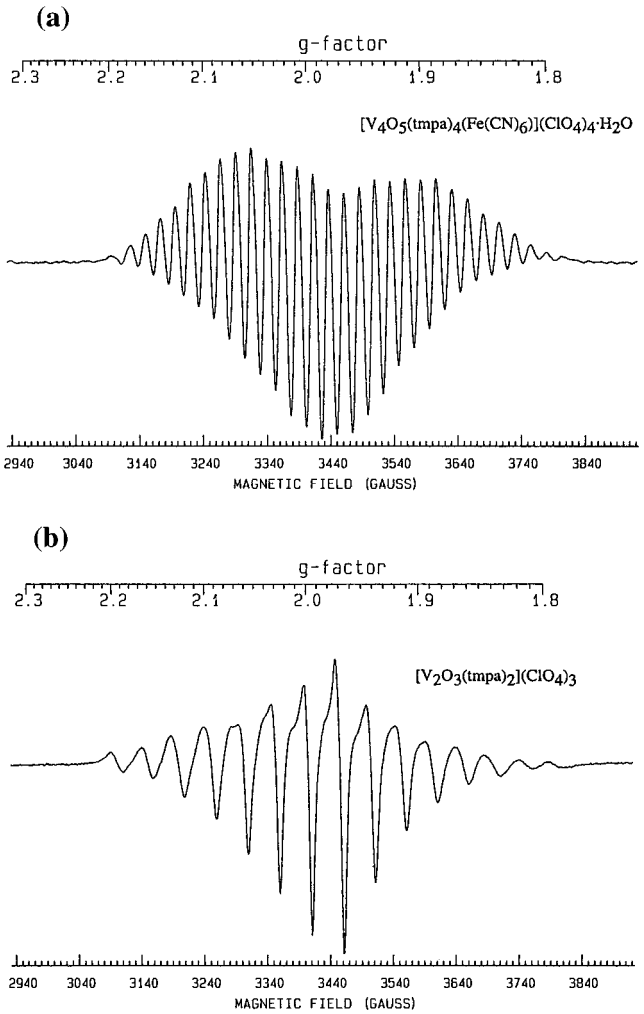

Figure 2. X-band EPR spectra of **2** (bottom, first derivative) and **4** (top, second derivative) in CH_3CN at ambient temperature.

The electronic spectra of **1** and **2** in a variety of solvents are recorded in Table 3. The mixed-valence complex has an intervalence transfer (IT) band at 1.05×10^4 cm^{-1} whose energy is insensitive to variations in the solvent. In addition, d−d transitions are observed at 1.25×10^4 cm^{-1} ($^2E \leftarrow {}^2B_2$) and 1.44×10^4 cm^{-1} ($^2B_1 \leftarrow {}^2B_2$). Complex **2** undergoes partial or full decomposition in some polar solvents, including water, DMF, and DMSO. However, a solid dihydrate of **2** could be isolated from a concentrated solution in aqueous $LiClO_4$. The electronic spectrum of **2** bears a strong resemblance to that of $[V_2(nta)_2(O_3)]^{3-}$ in propylene carbonate; the latter's IT transition is red-shifted by 700 cm^{-1} while d−d bands are at 1.34×10^4 and 1.68×10^4 cm^{-1}.[2] In contrast, the monomeric V^{IV} species resulting from decomposition of **2** in DMSO exhibits only weak d−d bands at 1.36×10^4 and 1.82×10^4 cm^{-1}. A true Robin−Day class III species will exhibit no solvent dependence of the IT transition energy, while the IT bands of class II dimers are expected to correlate linearly with $1/D_{op} - 1/D_s$, where D_{op} and D_s are the optical and static dielectric constants of the medium.[12] We observed less than a 100 cm^{-1} variation (λ_{max} = 951−958 nm) in IT transition energies for six solvents covering a significant range of $1/D_{op} - 1/D_s$ values (0.387−0.538), fully consistent with an assignment of **2** to class III.

Complex **2** also exhibits a strong near-ultraviolet transition at 2.83×10^4 cm^{-1}, resolved as a shoulder on the tmpa ligand π−π^* absorption. We assign this band as oxygen to vanadium LMCT, considering that divanadium(V) complex **3** has a poorly

Table 3. Electronic Spectra of $[V_2(tmpa)_2(O)_3]^{2+}$ and $[V_2(tmpa)_2(O)_3]^{3+}$ [a]

	$[V_2(tmpa)_2(O)_3]^{2+}$		$[V_2(tmpa)_2(O)_3]^{3+}$	
solvent	$10^{-4}E_{max}$, cm^{-1}	$10^{-3}\epsilon_{max}$, $M^{-1}\ cm^{-1}$	$10^{-4}E_{max}$, cm^{-1}	$10^{-3}\epsilon_{max}$, $M^{-1}\ cm^{-1}$
acetone	1.87	9.3	1.05	
			1.25	
			1.44	
acetonitrile	1.88	10.0	1.05	2.1
			1.25	1.3
			1.44	1.0
n-butylnitrile	1.87	5.4		
dichloromethane	1.87			
dimethylacetamide	1.86	9.2		
	2.22	5.0		
dimethylformamide[b]	1.86	7.2	1.36	0.031
	2.22	3.9	1.84	0.056
dimethyl sulfoxide[b]	1.85	6.8	1.36	0.025
	2.21	3.7	1.82	0.014
ethanol	1.89			
methanol	1.90	5.4	1.05	
			1.45	
N-methylformamide	1.86	11.0		
nitrobenzene	1.83	7.9	1.04	
			1.24	
			1.44	
nitromethane	1.88	9.7	1.04	1.9
			1.25	1.2
			1.44	0.89
propylene carbonate	1.87	7.6	1.04	1.8
	2.23	4.2	1.25	1.1
			1.44	0.84
pyridine	1.84	8.8		
	2.22	4.8		
water	1.94	8.5		
	2.29	4.4		

[a] Spectra recorded at ambient temperature immediately after solutions were prepared. For $[V_2(tmpa)_2(O)_3]^{2+}$, tabulations do not include a poorly resolved shoulder near $1.8 \times 10^4\ cm^{-1}$ or a transition at ca. $2.2 \times 10^4\ cm^{-1}$ when not resolved as a peak. For $[V_2(tmpa)_2(O)_3]^{3+}$, a weak shoulder near $2.0 \times 10^4\ cm^{-1}$ is omitted and the UV region was quantitatively examined for CH_3CN only: a shoulder at $2.83 \times 10^4\ cm^{-1}$ with $\epsilon = 2.8 \times 10^3\ M^{-1}\ cm^{-1}$. Extinction coefficients are not reported for solvents in which the compounds are slightly soluble. [b] Spectra of $[V_2(tmpa)_2(O)_3]^{3+}$ reported for this solvent correspond to decomposition products.

resolved shoulder near 360 nm (CH_3CN) and no visible absorption bands. The spectrum of divanadium(IV) complex **1** contains intense visible transitions at 1.94×10^4 and $2.29 \times 10^4\ cm^{-1}$ (H_2O), of which only the former is clearly resolved in all solvents examined. These features have been assigned as either μ-oxo to vanadium(IV) or vanadium(IV) to pyridyl group charge transfer.[13] The former assignment can be ruled out by the observation that similar intense transitions were not observed at lower energies when the oxidation state of vanadium was increased from +4 to +5 in **2** and **3**. Toftlund and co-workers point out that the latter assignment is inconsistent with resonance Raman enhancement of the V−O−V asymmetric vibrational mode with 520 nm excitation.[13]

Oxo-bridged transition metal complexes typically exhibit strong electronic transitions associated with the MOM chromophore.[12,16] We previously utilized a correlation of transition energy with solvent optical dielectric constant to demonstrate that the strongest near-ultraviolet feature of $[Cr(tmpa)(NCS)]_2O^{2+}$ is a chromium(III) to oxygen MLCT band ($e_g-e_u^*$, $^1A_{2u}\leftarrow{}^1A_{1g}$) within the π molecular orbital manifold of the CrOCr group.[16]

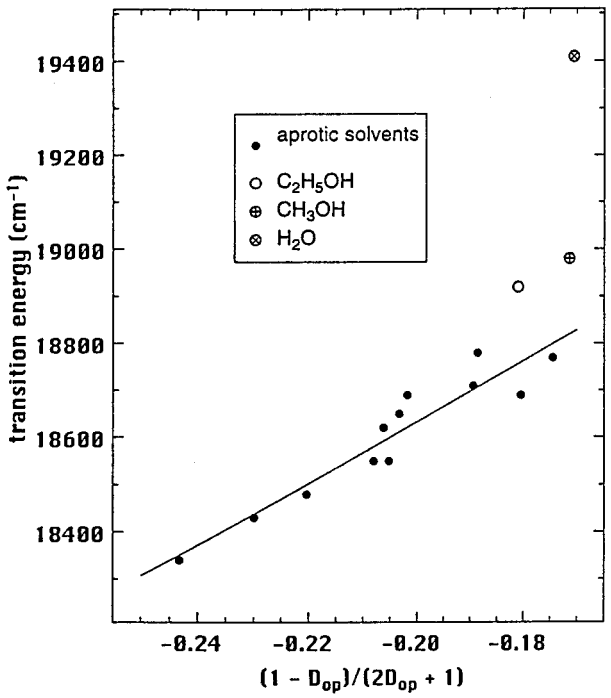

Figure 3. Correlation of transition energy with solvent optical dielectric constant for the most intense visible absorption band of **1**. Least-squares line includes points for aprotic solvents only.

Thus, Meyer and co-workers have shown that a MLCT transition to a localized ligand excited state should give rise to a linear plot of transition energy vs $(1 - D_{op})/(2D_{op} + 1)$[17] with a slope of μ^2/b^3, where μ and b are the dipole moment of the excited state and the chromophore radius, respectively. Figure 3 shows that such a correlation is also reasonably linear (excluding protic solvents) for the most intense electronic transition of **1** (slope $= 6520 \pm 710$), suggesting that this band could be assigned as an MLCT excitation of the VOV chromophore. On this basis, we estimate the radius of $[V(tmpa)(O)]_2O^{2+}$ at 3.97 Å (= sum of $V-O_b + V-N$ (trans to oxo) bond lengths)[13] and calculate $\mu = 9.0 \pm 1.0$ D, $b = 1.9 \pm 0.2$ Å. Strong splitting of the e_g (D_{4h}) molecular orbital in the pseudo-C_{2h} environment of the $V_2O_3^{2+}$ group could account for the diamagnetism[13] of **1**, in which two 3d electrons must be accommodated by a π molecular orbital.[16,18]

Beer's Law is followed by aqueous solutions of **1** (pH 6.0, $I = 0.1$ M ($NaNO_3$)) over the concentration range 8.0−160 μM (400−550 nm); there was no indication of a monomer−dimer equilibrium or a dimer decomposition reaction at ambient temperature. In contrast, dilute aqueous $[V_2(tmpa)_2(O)_3]^{3+}$ quickly undergoes hydrolytic oxo-bridge cleavage. A pH reading of 2.28 was recorded at equilibrium after 0.0727 g (68.3 μmol) of **2**·2H_2O was dissolved in 0.1 M $NaNO_3$ (10 mL). Loss of blue color and precipitation of a lavender product were accompanied by release of 69 μmol of H^+ according to the reaction

$$[V_2(tmpa)_2(O)_3]^{3+} + H_2O \rightarrow [V^{IV}(tmpa)(O)(OH)]^+ + [V^{V}(tmpa)(O)_2]^+ + H^+ \quad (1)$$

The electronic spectrum (DMF solution) of the quantitatively recovered V^{IV} product exhibited d−d transitions at $1.36 \times 10^4\ cm^{-1}$ ($\epsilon = 40\ M^{-1}\ cm^{-1}$) and $1.85 \times 10^4\ cm^{-1}$ ($\epsilon = 21\ M^{-1}$

(16) Gafford, B. G.; O'Rear, C.; Zhang, J. H.; O'Connor, C. J.; Holwerda, R. A. *Inorg. Chem.* **1989**, *28*, 1720.
(17) Kober, E.; Sullivan, B. P.; Meyer, T. J. *Inorg. Chem.* **1984**, *23*, 2098.
(18) Dunitz, J. D.; Orgel, L. E. *J. Chem. Soc.* **1953**, 2594.

cm^{-1}). $[V_2(tmpa)_2(O)_3]^{3+}$ hydrolysis was followed through loss of IT absorbance at 850 nm. Hydrogen ion and temperature dependences of k_{obsd} were evaluated in the ranges 0.2−100 mM (11 concentrations) and 10.9−45.2 °C (five temperatures), respectively (Figure 4 in Supporting Information). The hydrogen ion-independent rate constant, $k(25\ °C) = (2.37 \pm 0.02) \times 10^{-3}\ s^{-1}$, is governed by the activation parameters $\Delta H^{\ddagger} = 71 \pm 1$ kJ/mol and $\Delta S^{\ddagger} = -59 \pm 2$ J/mol K. These findings are consistent with an activated complex requiring both H_2O-V^{IV} bond-making and O_b-V^{IV} bond-breaking in the rate-limiting step.

An unexpected product was isolated from the reaction of **1** with equimolar $[Fe(CN)_6]^{3-}$ in aqueous solution. Although reactants were combined in a 2:1 V:Fe mole ratio, the corresponding ratio in product **4** is 4:1. Although $[V_4O_5(tmpa)_4\{Fe(CN)_6\}](ClO_4)_4 \cdot H_2O$ proved to be insufficiently stable for crystallization in both aqueous and nonaqueous media, our physical studies allow several structural conclusions to be drawn. Infrared features at 2056 and 981 cm^{-1} indicate the presence of a hexacyanoferrate(II) ion and vanadyl groups, respectively.[19,20] No reaction was noted between **1** and $[Fe(CN)_6]^{4-}$ in aqueous solution, while **4** formed immediately upon mixing $K_4[Fe(CN)_6] \cdot 3H_2O$ with **2** in 1:2 mole ratio. Complex **4** exhibits intense charge-transfer transitions at $1.98 \times 10^4\ cm^{-1}$ ($\epsilon = 5.3 \times 10^3\ M^{-1}\ cm^{-1}$) and $2.72 \times 10^4\ cm^{-1}$ ($\epsilon = 9.3 \times 10^3\ M^{-1}\ cm^{-1}$) ($CH_3CN$) but lacks the IT band observed for **2** at lower energy. A spectrophotometric titration of **1** against 0.10 mM $[Fe(CN)_6]^{3-}$ indicated that the $2.72 \times 10^4\ cm^{-1}$ feature is fully developed at a 1:1 (1.01 ± 0.03) mole ratio. The 29-line EPR spectrum of **4** (Figure 2, $g = 1.9737$, $A = 22.0 \times 10^{-4}\ cm^{-1}$ (66.0 MHz)) demonstrates equal delocalization of unpaired electron density over all four V atoms. Spin−spin coupling of the two $S = {}^1/_2$ units to give $S = 0$ and $S = 1$ states evidently is quite weak. Considering an ample precedent for the existence of mixed-valence $V^{IV/V}$−oxygen cluster complexes,[21,22] we propose that **4** contains pairs of $V^{IV}{=}O$ and $V^{V}{=}O$ units aggregated with $[Fe(CN)_6]^{4-}$ into a charge-transfer complex. The 1.98×10^4 and $2.72 \times 10^4\ cm^{-1}$ bands most likely correspond to IT charge transfer[12,23] from $[Fe(CN)_6]^{4-}$ $t_{2g}(\pi)$ into vanadium t_{2g} and e_g orbitals, respectively, analogous to the electronic spectrum of prussian blue.[11,24]

Acknowledgment. We thank the Welch Foundation for support of this research through grants to R.A.H. (D-735) and B.R.W. (D-1180). NIH Grant P-41-RRO1811 is acknowledged for the use of IERC resources.

Supporting Information Available: Tables of crystallographic data, atomic coordinates, anisotropic displacement factors, and bonding parameters for $[V_2(tmpa)_2(O)_3](ClO_4)_3 \cdot CH_3CN$ and Figure 4 illustrating hydrogen ion and temperature dependences of k_{obsd} for the acid hydrolysis reaction of **2** (10 pages). Ordering information is given on any current masthead page.

IC970983+

(19) Nakamoto, K. *Infrared Spectra of Inorganic and Coordination Compounds*, 2nd ed.; Wiley: New York, 1970.
(20) Czernuszewicz, R. S.; Nakamoto, K.; Okawa, H.; Kida, S. *Inorg. Chim. Acta* **1978**, *27*, L101.
(21) Suber, L.; Bonamico, M.; Fares, V. *Inorg. Chem.* **1997**, *36*, 2030.
(22) Karet, G. B.; Sun, Z.; Heinrich, D. D.; McCusker, J. K.; Folting, K. Streib, W. E.; Huffman, J. C.; Hendrickson, D. N.; Christou, G. *Inorg. Chem.* **1996**, *35*, 6450.
(23) Poulopoulou, V. G.; Taube, H. *Inorg. Chem.* **1997**, *36*, 2240.
(24) Robin, M. B. *Inorg. Chem.* **1962**, *1*, 337.